Accepted Manuscript

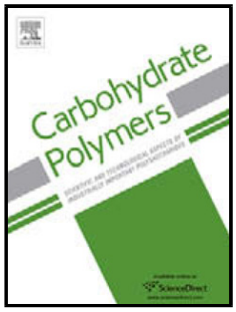

Title: Convenient characterization of polymers grafted on cellulose nanocrystals via SI-ATRP without chain cleavage

Authors: Zhen Zhang, Kam C. Tam, Gilles Sèbe, Xiaosong Wang

PII: S0144-8617(18)30851-8
DOI: https://doi.org/10.1016/j.carbpol.2018.07.060
Reference: CARP 13860

To appear in:

Received date: 13-4-2018
Revised date: 17-7-2018
Accepted date: 18-7-2018

Please cite this article as: Zhang Z, Tam KC, Sèbe G, Wang X, Convenient characterization of polymers grafted on cellulose nanocrystals via SI-ATRP without chain cleavage, *Carbohydrate Polymers* (2018), https://doi.org/10.1016/j.carbpol.2018.07.060

Convenient characterization of polymers grafted on cellulose nanocrystals via SI-ATRP without chain cleavage

Zhen Zhang[1,2], *Kam C. Tam*[3*], *Gilles Sèbe*[1,4*], *Xiaosong Wang*[2*]

[1]Université Bordeaux, LCPO, UMR 5629, F-33600 Pessac, France

[2]Department of Chemistry, Waterloo Institute for Nanotechnology, University of Waterloo, Waterloo, Ontario, Canada, N2L 3G1.

[3]Department of Chemical Engineering, Waterloo Institute for Nanotechnology, University of Waterloo, Waterloo, Ontario, Canada, N2L3G1

[4]CNRS, LCPO, UMR 5629, F-33600 Pessac, France

Graphical abstract

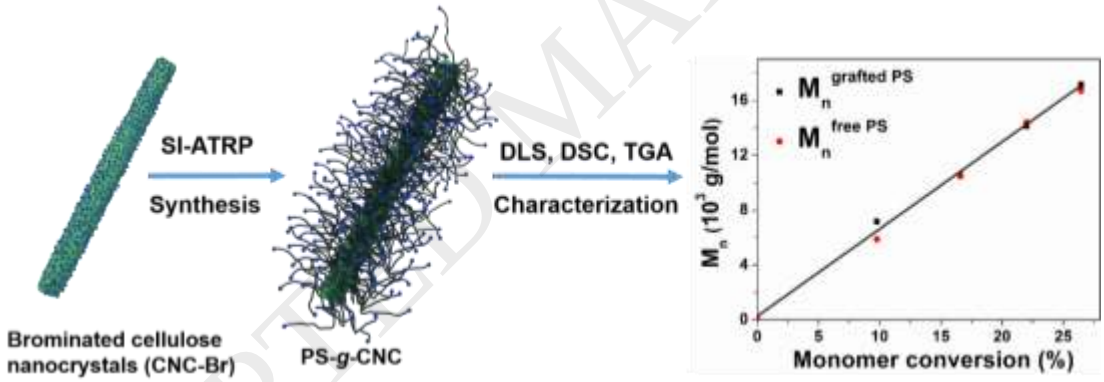

Highlights:

- Estimate M_n of grafted PS in PS-g-CNCs via TGA without chain cleavage
- Characterize PS-*g*-CNCs and free PS by FTIR, DLS, DSC, TGA, and GPC
- Grafting and free polymerization were progressing with similar propagating rates

Abstract

Cleaving is usually required to characterize the molecular weight of grafted polymers on substrates. Here, we report on a technique to estimate the molecular weight of grafted polystyrene (PS) ($M_n^{\text{grafted PS}}$) in PS-grafted cellulose nanocrystals (PS-*g*-CNCs) without chain cleavage. PS-*g*-CNCs were prepared from brominated CNC (CNC-Br) by Surface-Initiated Atom Transfer Radical Polymerization (SI-ATRP) in the presence of sacrificial initiators. Differential scanning calorimetry (DSC), dynamic light scattering (DLS), and thermogravimetric analysis (TGA) of PS-*g*-CNCs revealed that $M_n^{\text{grafted PS}}$ increased proportionally with monomer conversion. By comparing the mass of grafted PS, deduced from TGA curves, with initiating sites on CNC-Br, $M_n^{\text{grafted PS}}$ was calculated. The resultant $M_n^{\text{grafted PS}}$ was the same as M_n of free PS initiated by sacrificial initiators and matched theoretical values calculated according to monomer conversion. Therefore, grafting polymerization from CNC-Br and free polymerization were progressing in a controlled manner with the same propagating rates.

Keywords: Cellulose nanocrystals; SI-ATRP; DLS; DSC; TGA; polystyrene

1. Introduction

The grafting of polymers on nanoparticles is a promising "bottom-up" strategy to prepare well-designed nanocomposites with controlled properties.(Nicole, Laberty-Robert, Rozes, & Sanchez, 2014) In the "grafting-to" method, a pre-synthesized and characterized

polymers are covalently attached to the nanoparticles, leading to a low grafting density due to high steric hindrance. This problem can be circumvented by using the "grafting-from" approach, also known as Surface-Initiated Polymerization (SIP), in which the polymerization of monomers is initiated from the surface of the nanoparticles.(Zuo et al., 2017) The SIP is generally preferred due to the much lower steric hindrance.(Huang, 2016) Surface-Initiated Atom Transfer Radical Polymerization (SI-ATRP) is one of the most popular SIP methods because of its living radical polymerization characteristics. SI-ATRP has been widely used to graft polymers onto silica and metal nanoparticles,(Yan et al., 2016) and it has been recently applied to cellulose nanocrystal (CNC), a promising bio-based and biocompatible material.(Wei & McDonald, 2016; Yin et al., 2016) CNCs are renewable nanoparticles that possess many potential applications, such as reinforcing agents,(Sirviö, Visanko, Heiskanen, & Liimatainen, 2016; Yin et al., 2016; Zhen Zhang, Sèbe, Wang, & Tam, 2018) stabilizers for metal nanoparticles,(Lokanathan, Uddin, Rojas, & Laine, 2014; Z. Zhang, Sebe, Wang, & Tam, 2018) colloid stabilizers of Pickering emulsions,(J. Tang, Berry, & Tam, 2016; Zhen Zhang, Tam, Wang, & Sèbe, 2018) etc. However, the engineering of innovative nanomaterials from CNCs generally requires a fine control of their surface properties by chemical modification. In this context, the CNCs modification via SI-ATRP grafting is particularly promising, as it allows the preparation of hybrid polymer-grafted CNCs (polymer-*g*-CNCs) with tailored properties.

The properties of the polymer-*g*-CNCs obtained depend both on the chain length of the polymer and grafting density, hence controlled polymerization and precise characterization of the grafted polymer chains are necessary.(Dang et al., 2013) However,

the characterization of the molecular weight of the grafted polymer ($M_n^{\text{grafted polymer}}$) is challenging and it generally requires the cleavage and subsequent analysis by Gel Permeation Chromatography (GPC), which is tedious and time-consuming.(Wang, Roeder, Whitney, Champagne, & Cunningham, 2015) The severe conditions used for the cleavage can also degrade the cellulosic material or denature the polymer, making subsequent analysis challenging.(Rosilo et al., 2014) In many cases, it is practically impossible to cleave grafted polymers in mild conditions without special modifications of nanoparticles.(Hansson, Antoni, Bergenudd, & Malmström, 2011; G. Morandi & Thielemans, 2012) Alternatively, a sacrificial initiator is introduced into the SIP medium to produce free polymers necessary for M_n characterization.(Majoinen et al., 2011; G. Morandi & Thielemans, 2012) This method is based on the assumption that the molecular weights of the grafted polymers and free polymers ($M_n^{\text{free polymer}}$) are identical.(Hansson, Antoni, Bergenudd, & Malmström, 2011; G. Morandi & Thielemans, 2012) However, the accuracy of this method remains controversial. Indeed, the SI-ATRP reaction is influenced by steric hindrance of the grafted polymers, which is related to the grafting density and morphology of the substrate.(Xue et al., 2013) The relationship between grafted and free polymers is therefore not straightforward and needs to be verified for each particular case. Techniques to evaluate the molecular weight of the grafted polymers via a direct characterization of the polymer-*g*-CNC material have not been reported previously and hence, it should be very beneficial for researchers working in this field. To explore the possibility of characterizing the $M_n^{\text{grafted polymer}}$ without chain cleavage, we reviewed several techniques on the determination of the length of grafted polymers. For example, the glass transition temperature (T_g) of polymer-grafted nanocomposites as

measured by differential scanning calorimetry (DSC) may vary with $M_n^{\text{grafted polymer}}$ according to free volume theory.(Fox & Flory, 1950; Rudnick, Taylor, Litt, & Hopfinger, 1979) The hydrodynamic radius (R_h) of nanoparticles determined by dynamic light scattering (DLS) is related to the chain length of grafted polymers.(Mazurowski et al., 2013) The mass of grafted polymers relative to the nanoparticles can be measured using thermogravimetric analysis (TGA), which is expected to increase proportionally to the chain length of grafted polymers. Particularly, TGA technique can be used to measure the precise $M_n^{\text{grafted polymer}}$ by comparing the mass of grafted polymers with the number of initiating sites. By taking advantage of these widely-used techniques, it is possible to establish a technique to evaluate $M_n^{\text{grafted polymer}}$ without chain cleavage.

Herein, we report on the characterization of PS-grafted CNCs (PS-*g*-CNCs) using DLS, DSC and TGA techniques, allowing the direct determination of $M_n^{\text{grafted PS}}$ without PS chain cleaving. PS-*g*-CNC was prepared from brominated CNC initiators (CNC-Br) using SI-ATRP in the presence of a sacrificial initiator. PS was selected as a model polymer, as its surface grafting by ATRP has been performed on a wide variety of substrates as documented in the literature. The DLS, DSC and TGA analyses suggested that the grafted PS persisted with the monomer conversion. Particularly, the $M_n^{\text{grafted PS}}$ could be quantified without chain cleavage by comparing the mass of grafted PS, deduced from the TGA curves, with the initiating sites on CNC-Br. The calculated $M_n^{\text{grafted PS}}$ was identical to the $M_n^{\text{free PS}}$ measured using GPC and consistent with the theoretical $M_n^{\text{free PS}}$, indicating similar propagating rate for both grafting polymerization from CNC-Br and controlled radical polymerization in the bulk. DLS, DSC and TGA

techniques provide a facile approach to estimate the $M_n^{\text{grafted polymer}}$ without chain cleavage.

2. Experimental Section

2.1 Materials. CNCs were purchased from the University of Maine, which were prepared by sulfuric acid hydrolysis. Acetic acid, CuBr, $CuBr_2$, ascorbic acid, N,N,N',N'',N''-pentamethyldiethylenetriamine (PMDETA), tris [2-(dimethylamino)ethyl]amine (Me_6TREN), calcium hydride, styrene, dimethylformamide (DMF), tetrahydrofuran (THF), diethyl ether, ethanol and other solvents were purchased from Sigma-Aldrich. Ethyl αbromoisobutyrate (EBiB) and αbromoisobutyryl bromide (BIBB) were purchased from Alfa Aesar. 4-dimethylaminopyridine (DMAP) and triethylamine (TEA) were purchased from Fisher. CuBr was purified by acetic acid at 80 $^{\circ}C$ under N_2 for 24 h, and then washed with acetic acid and dried under vacuum at 50 $^{\circ}C$. All the other chemicals were used as received.

2.2 Preparation of the brominated CNC nano-initiators: CNC-Br. BIBB was used to modify CNCs and prepare the brominated CNC nano-initiators (CNC-Br), later used to initiate the SI-ATRP reaction. Firstly, CNCs (500 mg) were dispersed in DMF (50 mL) by sonication. TEA (4 mL) and DMAP (2 g) were added to the suspension. The suspension was evacuated under vacuum and backfilled with argon three times. Then BIBB (4 mL) was added dropwise to the suspension in an ice bath. After 24 h, EtOH was added, and the CNC-Br was recovered by centrifugation. CNC-Br was Soxhlet extracted with THF for 2 days, then dialyzed with deionized H_2O for 6 days. Finally, CNC-Br was obtained by freeze-drying. CNC-Br (10 mg) was re-dispersed in THF by sonication

again, and the supernatant was dried and analyzed by ^{1}H NMR in CDCl3. The ^{1}H NMR results showed no residues were left.

2.3 Grafting PS from CNC-Br by SI-ATRP: PS-*g*-CNCs. In brief, the SI-ATRP of PS from CNC-Br was conducted at 100 °C, with the molar ratio of [Styrene]: [EBiB]: [CuBr]: [PMDETA]: [DMF] = 500: 1: 1: 1: 500. In detail, CuBr (72 mg) was transferred into the Schleck tube in the glove box. CNC-Br (50 mg) was dispersed in DMF (250 mmol) via sonication. Then styrene (250 mmol) and EBiB (0.5 mmol) were added to the suspension. After the suspension had been bubbled with argon for 20 min, the suspension was transferred to the Schleck tube under the protection of argon. The suspension was degassed by three freeze-pump-thaw cycles. After the addition of PMDETA (0.5 mmol) under Ar, the reaction was initiated at 100 °C. At a designed interval time (2 h, 4 h, 6 h, and 7.3 h), an amount of reaction mixture was withdrawn by a degassed syringe. The monomer conversion was calculated from the ^{1}H NMR analysis of the mixture in $CDCl_3$. The mixture was centrifuged to recover the PS-*g*-CNCs nanoparticles. PS-*g*-CNCs were washed with THF and EtOH three times respectively, to remove the free polymer and other unreacted chemicals. In the last washing cycle, the THF supernatant was recovered and dried. The ^{1}H NMR of the dried supernatant in $CDCl_3$ showed no PS or other residues. The PS-*g*-CNCs nanocomposites were obtained after drying at 50 °C under vacuum. The green supernatant became colorless after the catalyst was removed in an Al_2O_3 column. The colorless supernatant was then poured into excess MeOH, and the precipitated free PS was recovered through filtration and drying at 50 °C under vacuum.

2.4 Characterization. Fourier transform infrared spectroscopy (FTIR) spectra of all the samples were obtained with the potassium bromide technique, using a Thermo Nicolet Avatar 970 FTIR spectrometer, at a resolution of 8 cm^{-1} (64 scans). Transmission electron microscopy (TEM) was conducted on Philips CM10 at an acceleration voltage of 60 keV. The TEM samples were prepared by drop coating the dispersion onto copper grids (200 mesh coated with copper) and

allowing them to dry at ambient temperature overnight. The pristine CNCs dispersion for TEM samples was stained by $FeCl_3$. Thermogravimetric analysis (TGA) was performed on TGA-Q50 system (TA Instruments) at a heating rate of 10 °C/min under nitrogen atmosphere. Differential scanning calorimetry (DSC) was carried out using a DSC Q100 apparatus (TA Instruments). All samples were first heated from 0 °C to 200 °C to remove the moisture, cooled down to 0 °C, and then heated to 200 °C. The T_g values were determined from the second heating run of the DSC curve. Dynamic light scattering (DLS) was performed using a particle size analyzer Vasco™ DL135 (Cordouan Technologies). Gel Permeation Chromatography (GPC) analysis was conducted in THF with LiBr, on a PL-GPC 50 plus Integrated GPC (Polymer Laboratories-Varian). The elution of the filtered samples was monitored using a simultaneous refractive index and UV detection system. The elution times were converted to molar mass using a calibration curve based on low dispersity (M_w/M_n) polystyrene standards. ^{1}H NMR spectra were recorded using a Bruker AC-400 NMR at room temperature by dissolving the samples in $CDCl_3$. Elemental analysis (EA) data were obtained from SGS Multilab. Carbon, hydrogen, and nitrogen were measured by thermal conductivity, according to protocols MO 240 LA 2008 (carbon and hydrogen) and MO 150 LA 2007 (nitrogen). Oxygen and sulfur were measured with infrared detectors, according to protocols MO 238 LA 2008 (oxygen) and MO 240 LA 2008 (sulfur). Bromide was measured by ionic chromatography, according to protocol MLE-MO-LAB-O78. All samples were dried at 105 °C before analysis.

3. Results and Discussion

3.1 Preparation and characterization of the CNC-Br initiator.

The CNCs used in this study were isolated via sulfuric acid hydrolysis of wood pulp, according to a general procedure widely described in the literature.(Beck-Candanedo, Roman, & Gray, 2005) As shown in Scheme 1, a widely reported esterification method with BIBB as reactant was employed to anchor Br initiating sites on the surface of the CNCs.(Hansson, Antoni, Bergenudd,

& Malmström, 2011) The successful preparation of CNC-Br was confirmed by FTIR spectroscopy (See Figure S1 in the supporting information) and ^{13}C CP-MAS NMR spectroscopy (Figure S2). The morphologies of pristine CNCs and CNC-Br were investigated by TEM (Figure S3). After modification by BIBB, CNC-Br retained the rod-like morphology. The thermal stability of the pristine CNCs and CNC-Br was investigated by TGA (Figure S4). Compared to pristine CNC, CNC-Br displays a reduction in the thermal stability. This result should be related to the presence of labile bromine within CNC-Br, which may accelerate the degradation of cellulose through free radical mechanisms or by forming HBr upon heating.(Sui et al., 2008)

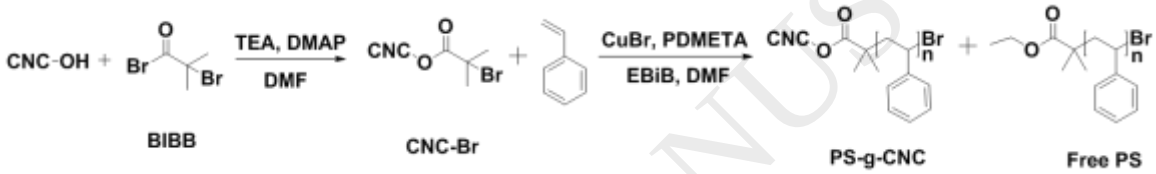

Scheme 1. Synthetic route used for the preparation of the PS-*g*-CNC and free PS

The bromine content in CNC-Br, evaluated by elemental analysis (EA) was estimated to be 11.9 wt. % (other elements: C 42.7 wt. %, O 34.3 wt. %, and H 5.2 wt. %). The EA results also confirmed the successful anchoring of Br initiator sites on the CNC. Based on the Br content, the molecular ratio of anhydroglucose relative to the grafted Br was estimated to be 3.2, using a method reported in the literature.(Majoinen et al., 2011) The detailed calculation is described in the supporting information. Hence, the molecular composition of CNC-Br can be simplified as $(C_6H_{10}O_5)_{3.2}(C_4H_6OBr)$. If necessary, the amount of initiating Br sites can be finely tuned by controlling the reaction conditions with BIBB.(Gaelle Morandi, Heath, & Thielemans, 2009)

3.2 SI-ATRP grafting of PS from CNC-Br

The ATRP grafting of PS from CNC-Br was performed in DMF, in the presence of ethyl α-bromoisobutyrate (EBiB) as sacrificial initiator (Scheme 1). The successful grafting of PS from CNC-Br was confirmed by the FTIR spectroscopy, as shown in Figure S1. Aliquots were taken at

designed polymerization intervals and analyzed by ^{1}H NMR, to evaluate the monomer conversion with time. The monomer conversion was calculated based on the ratio of styrene to DMF in the aliquots. The ^{1}H NMR spectra of the aliquots in $CDCl_3$ with different polymerization time are shown in Figure S5. The free PS and PS-*g*-CNCs in the aliquots were separated by centrifugation. The monomer conversion is given by $([M_0]-[M_t])/[M_0]$, where $[M_0]$ and $[M_t]$ are the monomer concentration at initial and time t, respectively.

The kinetic parameters are summarized in Table 1, and the monomer conversion and $\ln([M_0]/[M_t])$ were plotted as a function of reaction time in Figure 1. The monomer concentration decreased with time, leading to a gradual reduction in the propagation rate $R_p = K_p[M_t][P_n^*]$. Consequently, the increase in monomer conversion with time displayed a convex shape. The $\ln([M_0]/[M_t])$ increased linearly with time, suggesting a first-order kinetic reaction with a constant concentration of radicals, which is characteristic of a well-controlled ATRP process.(Matyjaszewski & Xia, 2001) The number-average molecular weight ($M_n^{\text{free PS}}$) and dispersity of free PS at different polymerization times, were evaluated by GPC. $M_n^{\text{free PS}}$ increased proportionally with respect to the monomer conversion, and the dispersity values remain below 1.15 (1.06-1.13), further confirming that the PS polymerized according to a “living” polymerization process. As the amounts of initiating sites on CNC-Br is negligible compared to the amount of sacrificial initiator, a theoretical $M_n^{\text{free PS}}$ value could be calculated based on the monomer conversion and molar ratio of monomer to initiator.

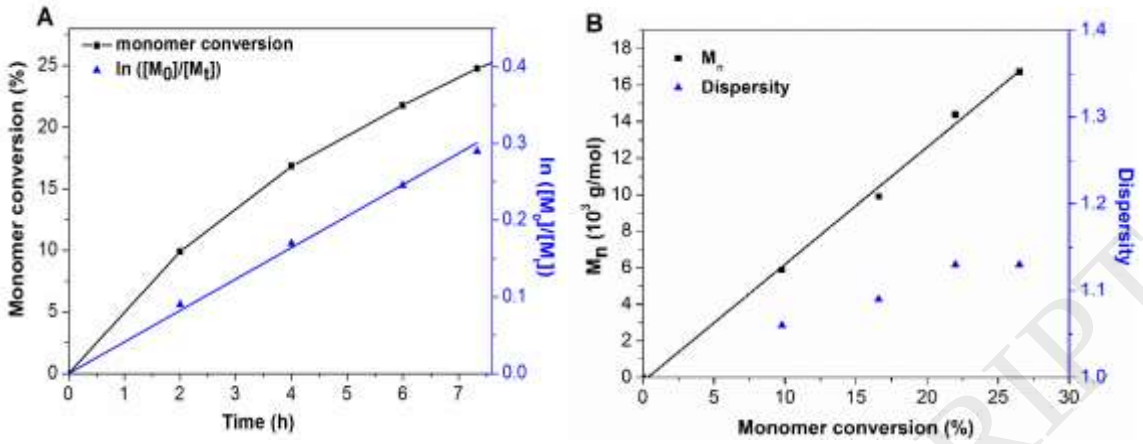

Figure 1. Kinetics of the ATRP polymerization of free PS: (A) Monomer conversion and $\ln([M_0]/[M_t])$ *vs.* reaction time; (B) M_n and dispersity of free PS *vs.* monomer conversion.

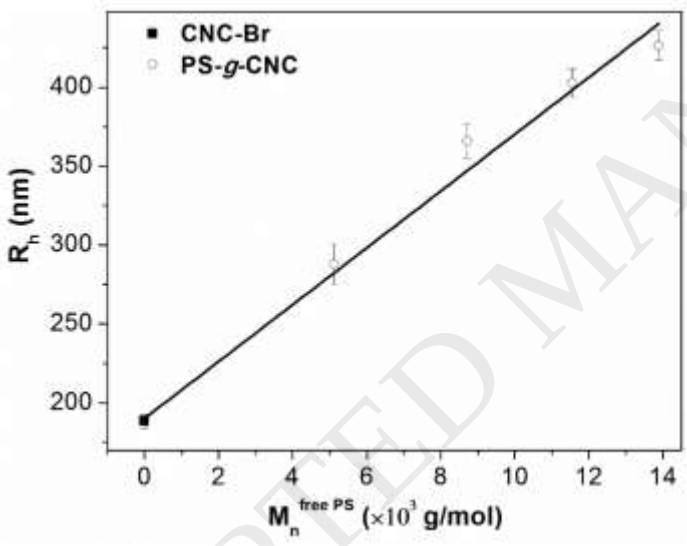

Figure 2. Evolution of the hydrodynamic radius (R_h) of PS-*g*-CNCs as a function of $M_n^{\text{free PS}}$.

The hydrodynamic radius (R_h) of the polymer-grafted nanoparticles measured by DLS, can be used to monitor the ATRP process.(van Ravensteijn & Kegel, 2016; Yan et al., 2016) The R_h only provides an indication of the apparent size of the nanoparticles.(Wang et al., 2015) It is expected that the R_h would increase correspondingly with the growth of the grafted PS chains.(J. O. Zoppe et al., 2016) The R_h of the PS-*g*-CNCs dispersed in THF was then measured by DLS and plotted as a function of the $M_n^{\text{free PS}}$ in Figure 2. Results indicate that the size of the PS-*g*-CNCs remained in the nanometer range. Zoppe et al. also reported a fairly large R_h for polymer grafted CNCs

which were also prepared by SI-ATRP.(J. O. Zoppe et al., 2016) The large R_h of PS-*g*-CNCs is due to the mild aggregation of the nanoparticles. The R_h increased linearly with $M_n^{\text{free PS}}$, suggesting the polymer at the CNCs surface grew at the same speed as the free polymer ($M_n^{\text{grafted PS}}$ increased linearly with the $M_n^{\text{free PS}}$). Since DLS is easy to perform, it can be used as a practical tool to monitor the polymerization process at the CNCs surface. However, the actual $M_n^{\text{grafted PS}}$ value cannot be obtained using this technique.

The glass transition temperatures (T_g) of free PS ($T_g^{\text{free PS}}$) and PS-*g*-CNCs ($T_g^{\text{PS-}g\text{-CNC}}$) were measured by DSC at different polymerization times. As shown in Figure 3A, both $T_g^{\text{free PS}}$ and $T_g^{\text{PS-}g\text{-CNC}}$ increased as the polymerization time was increased, while no T_g was observed for the CNC-Br. According to the free volume theory proposed by Fox and Flory,(Fox & Flory, 1950; Rudnick et al., 1979) the T_g of the polymer should increase proportionally to $1/M_n$ due to the decrease of free volume, following the empirical equation:

$$T_g = T_g^{\infty} - K_g/M_n,$$

where T_g^{∞} refers to the T_g of PS with infinite M_n and K_g is an empirical constant of the polymer.(Fragneaud, Masenelli-Varlot, Gonzalez-Montiel, Terrones, & Cavaillé, 2008) The linear correlation between T_g and $-1/M_n$ was confirmed for the free polymer in Figure 3B. Moreover, the $T_g^{\text{PS-}g\text{-CNC}}$ also increased linearly with $-1/M_n^{\text{free PS}}$, suggesting that the $M_n^{\text{grafted PS}}$ is proportionally to the $M_n^{\text{free PS}}$. However, we were unable deduce the precise $M_n^{\text{grafted PS}}$ value from these data. The $T_g^{\text{PS-}g\text{-CNC}}$ is higher than the corresponding $T_g^{\text{free PS}}$, especially in the low M_n range, which is consistent with the T_g of PS grafted SiO_2.(Dang et al., 2013) The higher T_g of PS-*g*-CNCs results from the increased steric hindrance after grafting.

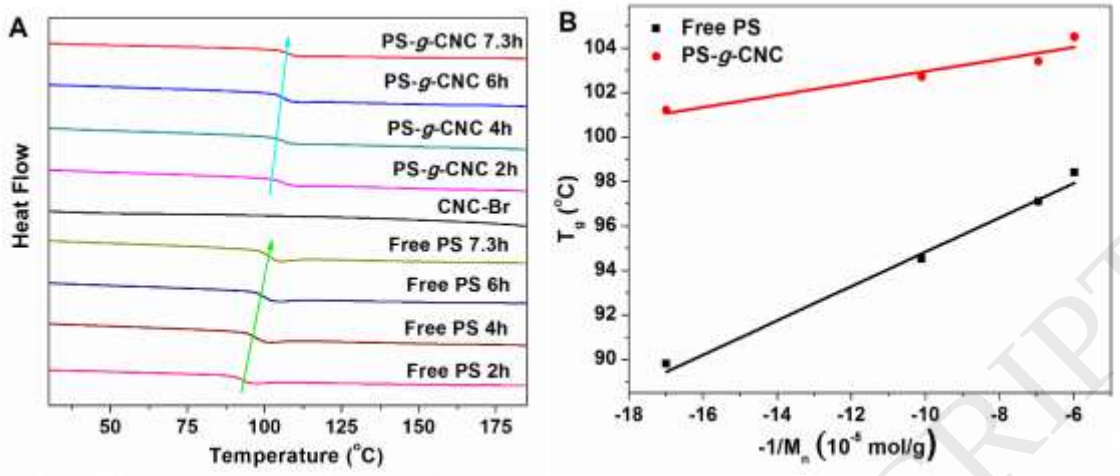

Figure 3. (A) DSC curves of CNC-Br, free PS, and PS-*g*-CNCs at different polymerization time; (B) T_g of free PS and PS-*g*-CNCs as a function of $-1/M_n^{\text{free PS}}$.

The thermal stability of free PS and PS-*g*-CNCs samples was evaluated by TGA, for different polymerization times. The thermograms and corresponding DTG derivatives of the free PS are shown in Figure 4A and B. The onset degradation temperature (T_{onset}) of the free PS increased slightly with reaction time, *i.e.* with increasing M_n. The main decomposition temperature of PS is in the range between 350 and 450 °C, which accounts for more than 95% of the PS weight loss. The TGA thermograms and DTG curves of PS-*g*-CNCs are shown in Figure 4C and D. The PS-*g*-CNCs displayed an enhanced thermal stability and possessed two stages of thermal transitions, which is consistent with literature data.(Yi, Xu, Zhang, & Zhang, 2008) The first weight loss (from 180 to 320 °C) is associated with the degradation of CNCs and the second weight loss (from 350 to 450 °C) with the degradation of PS. The ratio of second weight loss relative to first weight loss should then represent an accurate estimation of the weight ratio (R_w) of grafted PS to CNC substrate in the PS-*g*-CNCs. This ratio was plotted as a function of the monomer conversion in Figure 5. The linear correlation obtain suggests that the $M_n^{\text{grafted PS}}$ increased proportionally with respect to the monomer conversion.

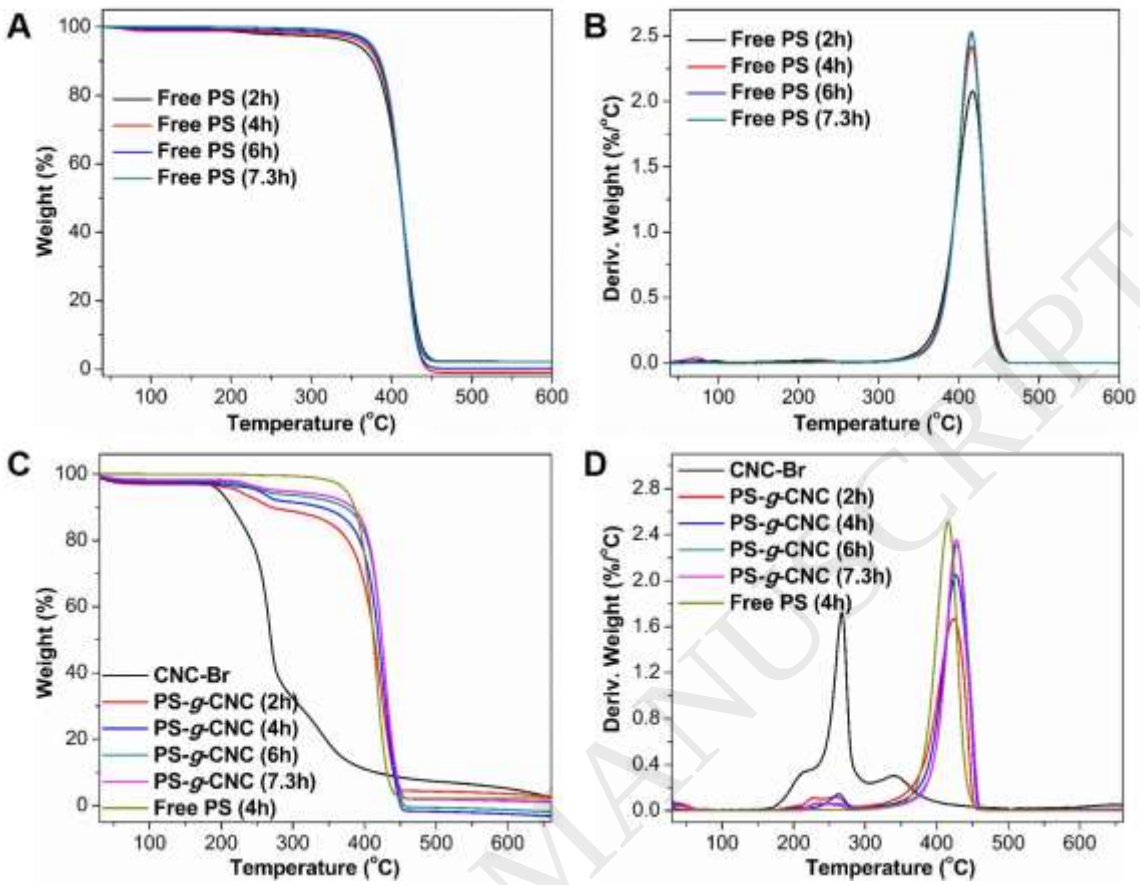

Figure 4. TGA thermograms and DTG curves of free PS (A, B) and PS-*g*-CNCs (C, D), respectively.

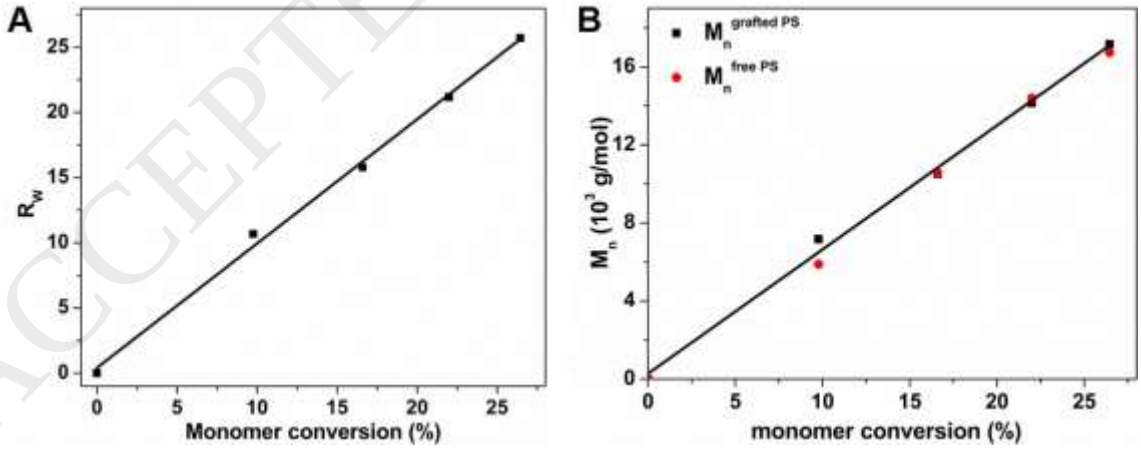

Figure 5. (A) Evolution of the weight ratio of grafted PS relative to CNC substrate in PS-*g*-CNCs (calculated by TGA) as a function of monomer conversion. (B) The $M_n^{grafted\ PS}$ derived by TGA and the $M_n^{free\ PS}$ measured by GPC

By comparing the weight of the grafted polymers with the number of initiating sites on CNC-Br, the exact $M_n^{\text{grafted PS}}$ can be calculated. Assuming that all Br sites on CNC-Br have reacted, the $M_n^{\text{grafted PS}}$ in PS-*g*-CNCs after 2h reaction was calculated as an example in the supporting information. The calculated $M_n^{\text{grafted PS}}$ values of the PS-*g*-CNCs samples obtained at different polymerization times were compared to the M_n values of the free polymers in Table 2. The $M_n^{\text{grafted PS}}$ derived from the thermal analysis agreed quite well with the $M_n^{\text{free PS}}$ measured by GPC. Due to the steric hindrance, the grafted polymer should exhibit similar or shorter polymer chain than the free polymer. If only part of Br sites on CNC-Br were initiated, the calculated $M_n^{\text{grafted PS}}$ will be larger than $M_n^{\text{free PS}}$. Therefore, the assumption that all Br sites on CNC-Br were initiated by SI-ATRP is reasonable. Both $M_n^{\text{grafted PS}}$ and $M_n^{\text{free PS}}$ increased linearly with the monomer conversion, confirming that the polymerization rates of the grafted and free polymers are identical. These results are consistent with previous reports performed on systems by cleaving the grafted polymer chain.(Hansson, Antoni, Bergenudd, & Malmström, 2011; G. Morandi & Thielemans, 2012) Therefore, the characterization of the free polymer is a convenient way to estimate the molecular weight of the polymer grafted on CNC-Br by SI-ATRP.

With the help of TGA, a correlation between the $M_n^{\text{grafted PS}}$ calculated from TGA and R_h or T_g of PS-*g*-CNCs could be obtained and used as a calibration curve for the same system. Therefore, DLS and DSC could be used to directly determine the $M_n^{\text{grafted PS}}$. As DLS is simpler to conduct than TGA, and it will be convenient to perform DLS instead of TGA, especially during the process of ATRP. We have attempted, but we failed to cleave the grafted PS from PS-*g*-CNC under an acidic condition at 75 $^{\circ}$C for 3 days. Other researchers have also reported that they failed to cleave the grafted polymer from cellulose under either acidic or basic condition.(Bontempo et al., 2006; Carlmark & Malmström, 2003; Ma et al., 2010; Östmark, Harrisson, Wooley, & Malmström, 2007; Sui et al., 2008) This difficulty in the chain cleavage justifies the importance

of the work described in this study. The proposed method is especially useful for the characterization of polymer-grafted nanoparticles when polymer cleavage is not feasible.

The proposed method is applicable for grafted polymer chains that exhibit different decomposition temperatures as CNC, and whose grafting density is known. The majority of the polymers that have been grafted onto CNC exhibit higher decomposition temperature than CNC as reported in the literature. Many polymers have been grafted on CNCs via different methods, such as PS,(Yi et al., 2008; Yin et al., 2016), poly(methyl acrylate),(Wang et al., 2015) poly(N-isopropylacrylamide),(Justin O. Zoppe, Österberg, Venditti, Laine, & Rojas, 2011) poly[2-(dimethylamino) ethyl methacrylate],(Rosilo et al., 2014), poly(n-butyl acrylate)(Majoinen et al., 2011), poly(4-vinyl pyridine),(Kan, Li, Wijesekera, & Cranston, 2013) poly(oligo (ethylene glycol) methacrylate),(Grishkewich, Akhlaghi, Zhaoling, Berry, & Tam, 2016) poly(methyl methacrylate),(Hansson, Antoni, Bergenudd, & Malmstrom, 2011) poly(6-[4-(4-methoxyphenylazo) phenoxy] hexyl methacrylate) poly(oxyethylene),(Kloser & Gray, 2010) and polyethylene glycol.(H. Tang, Butchosa, & Zhou, 2015) The decomposition temperature ranges of all these grafted polymers could be separated with the CNC. Therefore, the method could be used for most of the polymer grafted CNC system.

4. Conclusions

We developed a convenient method based on DLS, DSC, and TGA to characterize the grafted PS on the CNC surface by SI-ATRP without cleaving the grafted polymers. The brominated CNC nanoinitiator (CNC-Br) was obtained by esterifying CNC with BIBB. The successful anchoring of Br on CNCs was confirmed by FTIR, ^{13}C NMR and EA. PS was then grafted from CNC-Br by SI-ATRP in the presence of sacrificial initiators to produce PS-*g*-CNCs with various PS chain lengths. DLS was shown to be a convenient tool to monitor the polymerization process through the measure of the hydrodynamic radius of the PS-*g*-CNCs, which was found to increase linearly with the molecular weight of the free polymer. The DSC curves of the PS-*g*-CNCs particles

revealed a linear relationship between the glass transition temperature of PS-*g*-CNCs and -1/M_n of the free polymer. This confirm that the molecular weight of the grafted PS is correlated to the molecular weight of the free PS. Finally, we developed an original method based on TGA, to directly estimate the molecular weight of the PS grafted at the surface of the CNCs without cleaving the polymer from the nanoparticle, by comparing the weight losses imparted to the cellulosic material and grafted PS. We found that the M_n of grafted and free PS are in agreement, confirming that the free polymer produced by the sacrificial initiator can be used to represent the PS grafted at the CNCs surface.

Acknowledgments

We wish to acknowledge the University of Waterloo, University of Bordeaux, IDS-FunMat program, European commission, and the NSERC for providing finical support. We are thankful to Jérémie Brand and Benjamin Dhuiège for the help of FTIR and ^{13}C NMR. We are also grateful to Xiaobo Hu for the help of ^{1}H NMR.

References

Beck-Candanedo, S., Roman, M., & Gray, D. G. (2005). Effect of reaction conditions on the properties and behavior of wood cellulose nanocrystal suspensions. *Biomacromolecules,* 6(2), 1048-1054.

Bontempo, D., Masci, G., De Leonardis, P., Mannina, L., Capitani, D., & Crescenzi, V. (2006). Versatile grafting of polysaccharides in homogeneous mild donditions by using atom transfer radical polymerization. *Biomacromolecules,* 7(7), 2154-2161.

Carlmark, A., & Malmström, E. E. (2003). ATRP grafting from cellulose fibers to create block-copolymer grafts. *Biomacromolecules,* 4(6), 1740-1745.

Dang, A., Hui, C. M., Ferebee, R., Kubiak, J., Li, T., Matyjaszewski, K., & Bockstaller, M. R. (2013). Thermal properties of particle brush materials: effect of polymer graft architecture on the glass transition temperature in polymer-grafted colloidal systems. *Macromolecular Symposia,* 331-332(1), 9-16.

Fox, T. G., & Flory, P. J. (1950). Second-order transition temperatures and related properties of polystyrene. I. influence of molecular weight. *Journal of Applied Physics,* 21(6), 581.

Fragneaud, B., Masenelli-Varlot, K., Gonzalez-Montiel, A., Terrones, M., & Cavaillé, J. Y. (2008). Mechanical behavior of polystyrene grafted carbon nanotubes/polystyrene nanocomposites. *Composites Science and Technology,* 68(15-16), 3265-3271.

Grishkewich, N., Akhlaghi, S. P., Zhaoling, Y., Berry, R., & Tam, K. C. (2016). Cellulose nanocrystal-poly(oligo(ethylene glycol) methacrylate) brushes with tunable LCSTs. *Carbohydrate Polymers,* 144, 215-222.

Hansson, S., Antoni, P., Bergenudd, H., & Malmstrom, E. (2011). Selective cleavage of polymer grafts from solid surfaces: assessment of initiator content and polymer characteristics. *Polymer Chemistry,* 2(3), 556-558.

Huang, C.-F. (2016). Surface-initiated atom transfer radical polymerization for applications in sensors, non-biofouling surfaces and adsorbents. *Polymer Journal,* 48(4), 341-350.

Kan, K. H. M., Li, J., Wijesekera, K., & Cranston, E. D. (2013). Polymer-grafted cellulose nanocrystals as pH-responsive reversible flocculants. *Biomacromolecules,* 14(9), 3130-3139.

Kloser, E., & Gray, D. G. (2010). Surface grafting of cellulose nanocrystals with poly(ethylene oxide) in aqueous media. *Langmuir,* 26(16), 13450-13456.

Lokanathan, A. R., Uddin, K. M. A., Rojas, O. J., & Laine, J. (2014). Cellulose nanocrystal-mediated synthesis of silver nanoparticles: role of sulfate groups in nucleation phenomena. *Biomacromolecules,* 15(1), 373-379.

Ma, L., Liu, R., Tan, J., Wang, D., Jin, X., Kang, H., Wu, M., Huang, Y. (2010). Self-assembly and dual-stimuli sensitivities of hydroxypropylcellulose-graft-poly(N,N-dimethyl aminoethyl methacrylate) copolymers in aqueous solution. *Langmuir : the ACS journal of surfaces and colloids,* 26(11), 8697-8703.

Majoinen, J., Walther, A., McKee, J. R., Kontturi, E., Aseyev, V., Malho, J. M., Ruokolainen, J., Ikkala, O. (2011). Polyelectrolyte brushes grafted from cellulose nanocrystals using Cu-mediated surface-initiated controlled radical polymerization. *Biomacromolecules,* 12(8), 2997-3006.

Matyjaszewski, K., & Xia, J. (2001). Atom transfer radical polymerization. *Chemical Reviews,* 101(9), 2921-2990.

Mazurowski, M., Sondergeld, K., Elbert, J., Kim, C. J., Li, J., Frielinghaus, H., Gallei, M., Stühn, B., Rehahn, M. (2013). Polystyrene brushes on fully deuterated organic nanoparticles by surface-initiated nitroxide-mediated radical polymerization. *Macromolecular Chemistry and Physics,* 214(10), 1094-1106.

Morandi, G., Heath, L., & Thielemans, W. (2009). Cellulose canocrystals grafted with polystyrene chains through surface-initiated atom transfer radical polymerization (SI-ATRP). *Langmuir,* 25(14), 8280-8286.

Morandi, G., & Thielemans, W. (2012). Synthesis of cellulose nanocrystals bearing photocleavable grafts by ATRP. *Polymer Chemistry,* 3(6), 1402.

Nicole, L., Laberty-Robert, C., Rozes, L., & Sanchez, C. (2014). Hybrid materials science: a promised land for the integrative design of multifunctional materials. *Nanoscale,* 6(12), 6267-6292.

Östmark, E., Harrisson, S., Wooley, K. L., & Malmström, E. E. (2007). Comb polymers prepared by ATRP from hydroxypropyl cellulose. *Biomacromolecules,* 8(4), 1138-1148.

Rosilo, H., McKee, J. R., Kontturi, E., Koho, T., Hytonen, V. P., Ikkala, O., & Kostiainen, M. A. (2014). Cationic polymer brush-modified cellulose nanocrystals for high-affinity virus binding. *Nanoscale,* 6(20), 11871-11881.

Rudnick, J., Taylor, P., Litt, M., & Hopfinger, A. (1979). Theory of free volume in polymers. *Journal of Polymer Science: Polymer Physics Edition,* 17(2), 311-320.

Sirviö, J. A., Visanko, M., Heiskanen, J. P., & Liimatainen, H. (2016). UV-absorbing cellulose nanocrystals as functional reinforcing fillers in polymer nanocomposite films. *J. Mater. Chem. A,* 4(17), 6368-6375.

Sui, X., Yuan, J., Zhou, M., Zhang, J., Yang, H., Yuan, W., Wei Y,, Pan, C. (2008). Synthesis of cellulose-graft-poly(N,N-dimethylamino-2-ethyl methacrylate) copolymers via homogeneous ATRP and their aggregates in aqueous media. *Biomacromolecules,* 9(10), 2615-2620.

Tang, H., Butchosa, N., & Zhou, Q. (2015). A transparent, hazy, and strong macroscopic ribbon of oriented cellulose nanofibrils bearing poly(ethylene glycol). *Adv Mater,* 27(12), 2070-2076.

Tang, J., Berry, R. M., & Tam, K. C. (2016). Stimuli-responsive cellulose nanocrystals for surfactant-free oil harvesting. *Biomacromolecules*, 17(5), 1748-1756.

van Ravensteijn, B. G. P., & Kegel, W. K. (2016). Versatile procedure for site-specific grafting of polymer brushes on patchy particles via atom transfer radical polymerization (ATRP). *Polym. Chem.,* 7(16), 2858-2869.

Wang, H., Roeder, R. D., Whitney, R. A., Champagne, P., & Cunningham, M. F. (2015). Graft modification of crystalline nanocellulose by Cu(0)-mediated SET living radical polymerization. *Journal of Polymer Science Part A: Polymer Chemistry,* 53(24), 2800-2808.

Wei, L., & McDonald, A. (2016). A Review on Grafting of Biofibers for Biocomposites. *Materials,* 9(4), 303.

Xue, Y., Zhu, Y., Quan, W., Qu, F., Han, C., Fan, J., & Liu, H. (2013). Polymer-grafted nanoparticles prepared by surface-initiated polymerization: the characterization of polymer chain conformation,

grafting density and polydispersity correlated to the grafting surface curvature. *Physical Chemistry Chemical Physics,* 15(37), 15356-15364.

Yan, J., Pan, X., Schmitt, M., Wang, Z., Bockstaller, M. R., & Matyjaszewski, K. (2016). Enhancing initiation efficiency in metal-free surface-initiated atom transfer radical polymerization (SI-ATRP). *ACS Macro Letters,* 5(6), 661-665.

Yi, J., Xu, Q., Zhang, X., & Zhang, H. (2008). Chiral-nematic self-ordering of rodlike cellulose nanocrystals grafted with poly(styrene) in both thermotropic and lyotropic states. *Polymer,* 49(20), 4406-4412.

Yin, Y., Tian, X., Jiang, X., Wang, H., & Gao, W. (2016). Modification of cellulose nanocrystal via SI-ATRP of styrene and the mechanism of its reinforcement of polymethylmethacrylate. *Carbohydr Polym,* 142, 206-212.

Zhang, Z., Sebe, G., Wang, X., & Tam, K. C. (2018). Gold nanoparticles stabilized by poly(4-vinylpyridine) grafted cellulose nanocrystals as efficient and recyclable catalysts. *Carbohydr Polym,* 182, 61-68.

Zhang, Z., Sèbe, G., Wang, X., & Tam, K. C. (2018). UV-Absorbing cellulose nanocrystals as functional reinforcing fillers in poly(vinyl chloride) films. *ACS Applied Nano Materials,* 1(2), 632-641.

Zhang, Z., Tam, K. C., Wang, X., & Sèbe, G. (2018). Inverse pickering emulsions stabilized by cinnamate modified cellulose nanocrystals as templates to prepare silica colloidosomes. *ACS Sustainable Chemistry & Engineering,* 6(2), 2583-2590.

Zoppe, J. O., Österberg, M., Venditti, R. A., Laine, J., & Rojas, O. J. (2011). Surface interaction forces of cellulose nanocrystals grafted with thermoresponsive polymer brushes. *Biomacromolecules,* 12(7), 2788-2796.

Zoppe, J. O., Xu, X., Kanel, C., Orsolini, P., Siqueira, G., Tingaut, P., Zimmermann, T., Klok, H. A. (2016). Effect of Surface Charge on Surface-Initiated Atom Transfer Radical Polymerization from Cellulose Nanocrystals in Aqueous Media. *Biomacromolecules,* 17(4), 1404-1413.

Zuo, B., Zhang, S., Niu, C., Zhou, H., Sun, S., & Wang, X. (2017). Grafting density dominant glass transition of dry polystyrene brushes. *Soft Matter,* 13(13), 2426-2436.

Samples (Polymerization time h)	Monomer conversion (%)	$\ln([M_0]/[M_t])$	Theoretical M_n $^{\text{free PS}}$ (g/mol)	$M_n^{\text{free PS}}$ measured by GPC (g/mol)
Free PS (2h)	9.77	0.09	5128	5886
Free PS (4h)	16.60	0.17	8713	10575
Free PS (6h)	22.00	0.24	11546	14389
Free PS (7.3h)	26.45	0.29	13886	16732

Table 1. Kinetics parameters of the ATRP polymerization of free PS.

Samples (polymerization time)	$M_n^{\text{free PS}}$ measured by GPC (g/mol)	R_w measured by TGA	$M_n^{\text{grafted PS}}$ (g/mol)
PS-*g*-CNCs (2h)	5886	10.69	7140
PS-*g*-CNCs (4h)	10575	15.80	10554
PS-*g*-CNCs (6h)	14389	21.18	14148
PS-*g*-CNCs (7.3h)	16732	25.72	17181

Table 2. $M_n^{\text{free PS}}$ and $M_n^{\text{grafted PS}}$ values of the PS-g-CNCs obtained at different polymerization times.